Chem Soc Rev

Metal-organic molecular cages: Applications of biochemical implications

Journal:	*Chemical Society Reviews*
Manuscript ID:	CS-TRV-07-2014-000222.R2
Article Type:	Tutorial Review
Date Submitted by the Author:	02-Jul-2014

Complete List of Authors:	Ahmand, Nazir; Wuhan University of Technology, State Key Laboratory of Advanced Technology for Materials Synthesis and Processing Younus, Hussein; Wuhan University of Technology, State Key Laboratory of Advanced Technology for Materials Synthesis and Processing; Fayoum University, Chemistry Chughtai, Adeel; Wuhan University of Technology, State Key Laboratory of Advanced Technology for Materials Synthesis and Processing verpoort, francis; Wuhan University of Technology, State Key Laboratory of Advanced Technology for Materials Synthesis and Processing

Metal-organic molecular cages: Applications of biochemical implications

Nazir Ahmad[a,b], Hussein A. Younus[a,b,e], Adeel H. Chughtai[a,b,f], Francis Verpoort[a,b,c,d*]

[a] *Laboratory of Organometallics, Catalysis and Ordered Materials, State Key Laboratory of Advanced Technology for Materials Synthesis and Processing; Center for Chemical and Material Engineering, Wuhan University of Technology, Wuhan 430070, China.*
[b] *Department of Applied Chemistry, Faculty of Sciences, Wuhan University of Technology, Wuhan 430070, China.*
[c] *Tomsk Polytechnic University, Lenin Avenue 30, Tomsk 634050, Russia.*
[d] *Ghent University Global Campus Songdo, 119 Songdomunhwa-Ro,Yeonsu-Gu, Incheon 406-840, South Korea.*
[e] *Chemistry Department, Faculty of Science, Fayoum University, Fayoum 63514, Egypt.*
[f] *Institute of Chemical Sciences, Bahauddin Zakariya University, Multan 60800, Pakistan.*
[*] ***Corresponding author:*** *Tel.: +86 18701743583; Fax: +86 2787879468. E-mail: Francis.verpoort@ugent.be*

Abstract

New well-designed materials are highly demanded with the prospect of versatile properties, offering successful applications as alternates to conventional materials. Major new insights into metal-organic self-assembled structures assisting biochemical purposes have recently emerged. Metal-organic polyhedral cages are highlighted as new research materials to be used for therapeutic, sensing and imaging, *etc*. purposes. This tutorial review covers achievements in the biochemical applications of these multinuclear complexes. Examples of their ability to aid the ionic transport, biomolecular sensing, imaging, and drug delivery are presented.

1. Introduction

Material science has developed fascinating families of metal-organic materials (MOMs), *e.g.*, polygons, discrete polyhedral cage systems, and coordination polymers. The structural motif in these materials involves metal moieties (ions or clusters) coordinated by the polydentate organic bridging linkers. Based on the connectivity and geometry of the building components, materials of different and characteristic geometrical dimensions (0D (polygons and discrete polyhedra), 1D (chains, ladders and tapes), 2D (sheets and bilayers), and 3D extended networks) can be assembled.[1, 2]

Metal-organic frameworks (MOFs) are crystalline polymeric coordination networks, in which metal centers and ligands form repeating three dimensional architectures with potential inner porosity. The 3D extended networks of MOFs have uniform pore diameters (typically in the range 3 to 20 Å) with unprecedented internal surface areas (even higher than 7000 m^2g^{-1} with the theoretical upper limit for MOF surface areas 14600 m^2g^{-1} (or greater)), high void volumes (55–90%), and low densities (from 0.21 to 1.00 gcm^{-3}).[3] MOFs are attractive due to their unique and interesting solid frameworks, high surface area-to-weight ratio, structural tuning, convenient functionalization processes, robustness, and high thermal and chemical stabilities. Applications of MOFs are promising for gas storage and separation/purification, molecular sensing, drug delivery, and heterogeneous catalysis *etc.*[3-5]

Metal-organic polyhedra (MOPs) are discrete coordination self-assemblies having cage-like well-defined structures and confined cavities. Precious achievements in the technological developments based on the metal-organic formulations which are symmetrically self-assembled into discrete molecular architectures are attention grabbing. The phenomena of self-assembling, resulting in the highest degree of symmetry from a multiple number of subunits are frequently observed in biological systems, *e.g*., ferritin, capsid and tobacco mosaic virus are the self-assemblies of protein subunits deigning the polyhedral symmetry. Similarly, numerous abiological self-assembled discrete polyhedra have been made from metal ions and organic scaffolds. During the last decade significant progress in design and synthesis of metal-based capsules arose.[6] These cage-like macromolecules possess nanocavities with multiple open windows allowing small molecules to enter and pass through. A variety of metal-organic self-assembled cages have been introduced to encapsulate multiple numbers of guests supported by specific host-guest interactions and nonspecific supramolecular interactions *e.g.* Coulomb, Van

der Waals, hydrogen bonding, ion-association forces, and steric interactions. Additionally, the synergistic integration of charge, dielectric properties, shape, size, and solvation further reinforce the guest binding preferences in host cages. The passage, encapsulation, and/or binding of the guest species in the well-defined cage cavities are certainly responsible for the potential applications. MOPs are flexible in their topologies, sizes, surface areas, and porosities.[7] The spectrum of utility of MOPs can be extended based on the features like permanent porosity, highly selective guest binding/encapsulation, solubility, chemical and thermal stability *etc*.[8, 9] The use of host-guest chemical systems in catalysis and sorption based separations has been a popular subject. Recently, self-assemblies have attracted the attention for applications of the biochemical relevance. Hence, based on the structure and functions of molecular cages several biochemical investigations as ion channels, probes, molecular recognition and sensing, and drug delivery agents *etc.* are undergoing. Thus, numerous molecular architectures with specified modular polyhedral shapes along with sizes ranging from few cubic angstroms to over cubic nanometers have been reported.[7]

The study of biochemical applications of MOMs is at its developing stage. Recently, considerable progress has been made in this perspective. The exploration of such materials which provide functionality, durable stability, and biological compatibility is the forefront of technological developments in biophysical science through material research. Recently, MOFs have been reviewed for their biochemical and biomedical applications: these includes (i) the encapsulation or incorporation of biomolecules in the MOF structure (bio-MOF), (ii) biomimetic catalysis, (iii) biosensors, (iv) bioactive NO release, and (v) in biomedicines *etc*.[5, 10, 11] But, still there are several challenging issues to deal with (i) the stability in a physiological environment, and (ii) the development of new synthetic techniques in order to synthesize and crystallize

biocompatible MOFs, where the utilization of biomolecules with low symmetry, flexible structure, and limited solubility in common solvents are often unavoidable.[10] Further, the exhibition of high stability, large porosity, low cost are relatively rare. Recently, MOPs have been reported as an exciting family of supramolecular biomimetic materials for applications that have strong biochemical or biomedical relevance. For a practical utility of a cage with effective biochemical significance, it needs stability, congenial combination with the biological system, and proper operating mechanisms in given conditions of the hetero- or homogeneous and aqueous media. These features nominate MOPs for their potential applications in therapeutic, sensing and imaging. Similar to MOFs, MOPs have been reviewed for their structural design, synthesis, properties, and applications *e.g.,* catalytic and strategic building block for MOFs.[1, 2, 6, 12] Therefore, here we present a tutorial review on a new topic providing the recent developments of metal-organic molecular cages for the applications of biochemical implications, which is necessary in order to draw general conclusions and provide some guided perspectives for future research, despite the fact that a few related research articles involving related topic have appeared.

2. Metal-organic molecular cages

Metal-organic molecular cages, also called as supramolecular coordination self-assemblies are a class of chemically bonded hybrid materials. Unlike MOFs, MOPs are not infinite networks, but instead they are discrete metal-organic molecular entities, which are constructed from edge-sharing molecular polygons or *via* connections between molecular vertices (Fig. 1). This independent existence of a given polyhedral (platonic, Archimedean, faceted, and stellated) self-assembly makes MOPs as a different class of MOMs parallel to MOFs.[2] The network topologies of MOFs do exist when the points of extensions around the discrete polyhedral dimensions of

MOPs are allowed to further grow, *i.e.,* metallic nodes (vertices) with higher connectivity and/or polytopic organic spacers (faces). Therefore, MOPs as secondary building blocks (SBBs) could be exploited for generation of extended network of MOFs (Fig. 1).[1] More importantly, the perspective of soluble nature of given MOP cages which can exist in solution in equilibrium makes them distinctive materials to be used for certain applications in the homogeneous media in contrast to MOFs which mostly exist as insoluble crystalline solids. Further the advantage of the chemical stability in addition to solubility in different media for given MOP cages favors their use in the biochemical environments.[9]

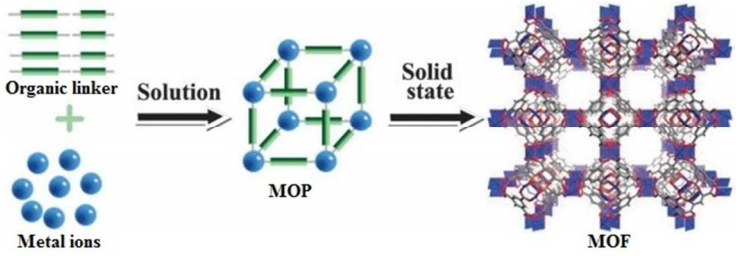

Fig. 1. Discrete Metal-organic polyhedra (MOP) and 3D framework (MOF). Reproduced from ref. 3.

The construction like capsules, boxes and polyhedral shapes with desired functions in a controlled manner is easily governed with the help of self-assembly principles. Large windows in the cages serve as the gateway passage for small molecules providing an opportunity to use them in the biophysical applications. The size and chemical environment of the cage periphery, cavity and windows are expected to be easily tuned by changing the metal ion and/or modifying the organic ligand organizing the framework. Resultantly, wide varieties of cage modulations are observed from the limitless combinations of ligands with metals. These cages are applied for various applications *e.g.* catalysis, molecular sensing, drug delivery, separation and purification. The physicochemical properties of metal-organic cages are controlled by the variation of metal centers and suitable functionalized ligands which tune the structures for the biochemical applications.[13, 14]

2.1. Design

Recently, numerous thematic reviews have discussed the vast progress in the design, and synthesis of these attractive materials.[2, 6, 7, 15, 16] Therefore, here it is not intended to present the design perspective in details, rather to overview some general design basis with more focusing to the most recent examples from those cage systems having biochemical implications. Several strategies are used to design the discrete metal-organic self-assemblies. These include directional bonding, symmetry interaction, molecular paneling, and reticular chemistry (using finite secondary building units (SBUs)) *etc*. The important parameters to design the geometry, size and function of the molecular cages are; the coordination geometry of the metal center, and the type and shape of the organic bridging linker. In account of these factors, different spherical or polyhedral cage geometries can be rationalized. Transition metal ions are commonly employed to construct the metal-organic polyhedral (MOPs) cages. In the foundation of cage assemblies, metals usually occupy the vertices. The metal center shows an important role to achieve the required properties and shape. Metal ions like Fe(II), Co(II), Ni(II), Cu(II), Zn(II) Mo(II), Ru(II), Rh(II), Pd(II), and lanthanides *etc*. have been used. The organization to obtain a cage is the function of bridging links. Multidentate ligands bearing different type of functionalities, *e.g.,* carboxylic, hydroxyl, nitrogen and/or Schiff base donor groups, *etc.*, bridge the geometrically pre-fixed metal nodes. The type and shape of the ligand, and its combination with given metal ions will decide the exact geometry of the cage.

A wide variety of interesting cage structures can be designed by the suitable combination of the building components (ligands and metal ions/clusters) possessing different connectivity. To overview the general design blueprints for the MOP generation, two main approaches are considered: edge-directed and face-directed (molecular paneling) (Fig. 2).[17] As an important

requisite for the polyhedral structure, at least one component of the systems must show a bent (θ < 180°) geometry. This provides the needed curvature for the formation of a finite symmetry. (i) Edge-directed approach involves the connection of ditopic edge components with the multitopic components at the corners of the polyhedron (Fig. 2a). Whereas, (ii) in the case of face-directed methodology, polytopic facial components are linked with the ditopic components or tritopic components at the edges (Fig.2b) or corners (Fig. 2c), respectively. The size and geometry of the self-assembly can be modulated accordingly with the control of the building components. Various combinations of the C_2, C_3, C_4, and C_5 symmetric components as edges, faces and corners can assume interesting MOP's symmetries. For the cubic symmetry, a C_3 symmetric component shows a key role. Thus, metal-organic cubical cages with *T*, *O*, and *I* symmetries result from the combinations of a C_3 symmetric building component with a component of C_2, C_4, and C_5 symmetry, respectively.

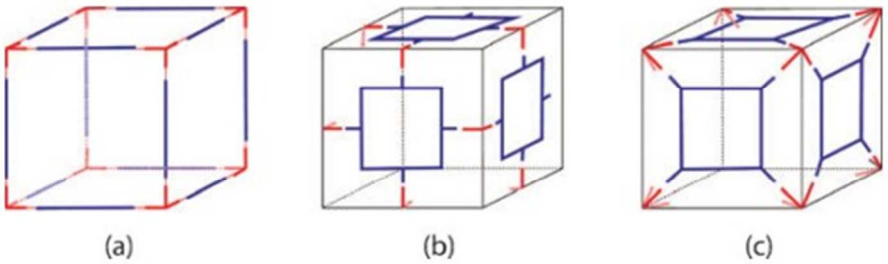

Fig. 2. (a) Linear ditopic edge components connected with C_3 symmetric corner components, (b) C_4 symmetric facial components connected with the bent ditopic edge components and (c) C_4 symmetric facial components connected with C_3 symmetric corner components. Reproduced from ref. 17.

Similarly, these approaches have been used to design a wide range of polyhedral cages having platonic dimensions and significantly larger structures like cuboctahedron (Archimedean) and so on. The MOP augmentation can be obtained when secondary building units (SBUs) are used as the building components of the MOPs as compared to primary building units. The paddlewheel (PW) cluster, $[M_2(COO\text{-})_4]$, serves as a square planar tetratopic SBU in the MOPs. A brief sketch about some selected examples of MOP cages is presented here.

In recent years, metal-organic tetrahedral container molecules have gained continuing growth as photo-reactors, stabilizing the reactive species, and functional mimics of biological molecules such as protein receptors and enzymes. The C_2-symmetric bis-bidentate ligands are extensively used as tetrahedral edges between four 6-coordinated transition metal(II) ions at the vertices. Nitschke and coworkers introduced tetrahedral cages and helicates from bis-bidentate pyridylimine (PI) ligands with divalent transition metal ions. Cages of Fe(II), Co(II), Cd(II), and Ni(II) offered selectivity in encapsulation of many small guest molecules. The thermodynamic and kinetic profiles for the guest binding, and diffusion/transport parameters are quite attractive under normal physiological conditions.[18-20]

The subcomponent self-assembling of the edge bridged tetrahedral Fe_4L_6 cages (having approximate *T* symmetry with either *mer*- or *fac*-configuration) are shown in Fig. 3. Cage Fe-PI1[19] occupied a lager guest-accessible void volume (*ca.* 245 Å^3) as compared to cage Fe-PI2[18] (*ca.* 136 Å^3). The externally-directed amine residues can be replaced to get a very large dynamic library from mixtures of amines. Therefore, these types of cages have displayed external selectivity, dynamic interchange demonstrated at the periphery through aniline substitution *i.e.* e^--rich amines can be incorporated relative to the e^--poor ones. The dynamically reconfigurable exterior provides a control over the cage solubility in a given system. The competitive incorporation of the organic subcomponent along with the guest (counter anion(s)) encapsulation would provide specific responses to the applied stimuli.[18, 19]

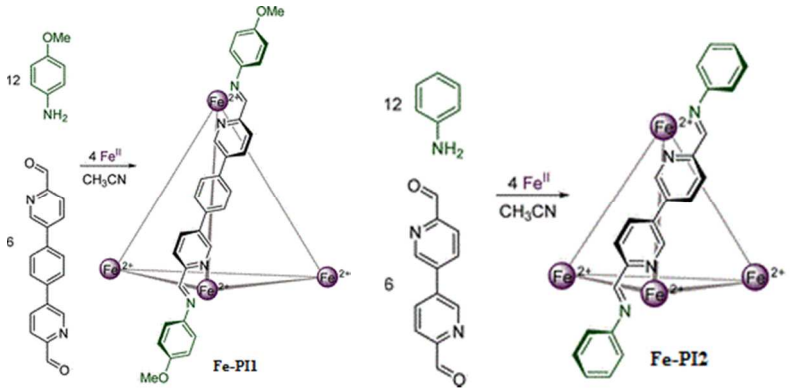

Fig. 3. Formation of cages Fe-PI from iron(II) and either 5,5′-(1,4-phenylene)bis-2-pyridinecarboxaldehyde and anisidine (Fe-PI1) or 6,6′-diformyl-3,3′-bipyridine and aniline (Fe-PI2). Reprinted with permission from ref. 19. Copyright 2013 American Chemical Society.

The C_3 symmetric ligands are utilized for designing tetrahedral cages by capping four faces of a tetrahedron. Tridentate coordinating ligands sharing a couple of five (or six) membered chelating rings have been established as efficient building blocks for the development of regular and highly symmetric lanthanide-based tetrahedra. These metaled cages are achieving prominence due to their promising functionalities as abiological host platforms and abilities to effectively bind substrates. Duan and coworkers have designed a variety of the lanthanide architectures by validating the face-driven strategy. The NOO incorporated chelator in a rationally designed ligand (H_6TTS) was used to get a Ce-H_2TTS tetrahedron (Fig. 4) in which the Ce···Ce distance was 14.9 Å. The inner volume of the cage cavity was about 360 Å^3, and has a crystallographic C_3 symmetry in the solid state. The rhombic window size dimensions were 6.5×6.5 Å^2. According to ^{1}H-NMR, beside the phenol groups, one third of the amide groups were also deprotonated. The hydrophilic/lipophilic environment due to amide groups within the cage is highly selective and sensitive for biological recognition and imaging.[21]

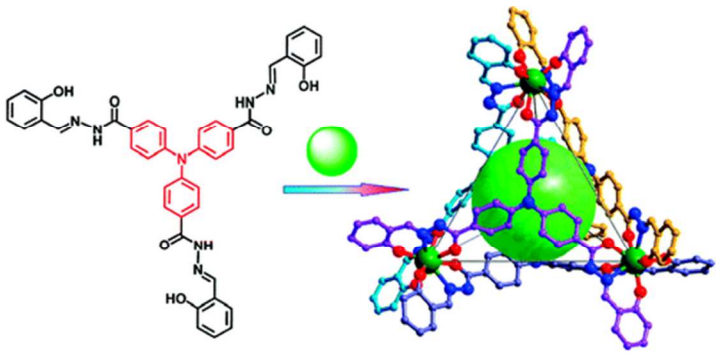

Fig. 4. Structure of H_6TTS, constitutive/constructional fragments of Ce-H_2TTS tetrahedron. Reprinted with permission from ref. 21. Copyright 2011 American Chemical Society.

The topology, size, and position of the weak interaction sites of cages can be tuned for developing efficient selective chemosensors. By introducing multiple amide groups, it is envisioned to have appropriate matches with the polar groups to address the structural diversity and favor the conformation for biomolecular recognition analysis. In this case, a size- or shape-selective dynamic molecular recognition system may accelerate detection and amplification of guest-binding events producing a measurable output. Therefore, a proper communicating system capable to transduce the recognition information into an easy-to-measure signal is necessary to include in the molecular design. The Ce-tetrahedral cages containing 24 amide groups have been characterized in this regard. The coordination with tridentate NOO chelators in a symmetrical coordination configuration can be used to prepare molecular cubes as well as octanuclear bicoronal triangular cages. Ligands TBDS and TBBS has been used with Ce(IV) to design the metal-organic cubes (Fig. 5), where each cerium site coordinates to three tridendate chelating groups.

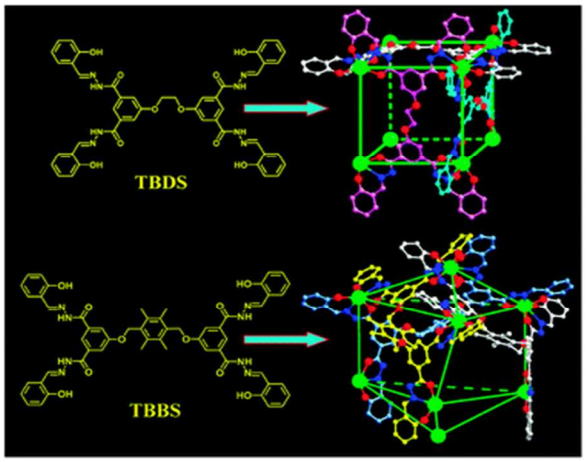

Fig. 5. Structures of Ce(IV)-based cubes using TBDS and TBBS. Reproduced from ref. 22.

In Ce-TBDS, the Ce···Ce separations are similar, ranging from 11.56 to 11.74 Å, so that *meso*-substituted benzene rings remain almost coplanar giving an overall regular cubic geometry. While, six connected TBBS ligands produce an octanuclear polyhedron with different bridging Ce···Ce separations (9.45 *vs* 19.55 Å) are obtained due to the larger spacer groups in TBBS compared with those in TBDS. Additionally the ligand flexibility, and π···π stacking interactions between the spacer rings direct the four cerium atoms to be connected into a twist configuration (Fig. 5). The cage volumes of Ce-TBDS and Ce-TBBS are 500 and 750 $Å^3$ with the opening diameters of 5 and 8 Å, respectively. These cage sizes and amide functionalities are suitable for the carbohydrate chemosensing.[22]

Several molecular octahedral nanocages of metal ions like Co(II), Ni(II), Zn(II), Pd(II), Eu(III), Tb(III) and Gd(III) *etc*. with the C_3-symmetric facial ligands have been established. The combination of amide, Schiff base and pyridine functional moieties in an NNO tridentate chelator is used to generate Warner-type capsules as metal-organic octahedra. The constitutive/ constructional fragments in the given octahedron are changed or modified to tune the structure. Cheng *et al.* described metal-variable isostructural nano-octahedral cages and reported them as chemosensors. The octahedral Gd(III)-PT1 cage is shown in Fig. 6. In the hexanuclear cage, four ligands are alternatively positioned on the four triangular faces. Each Gd-ion is coordinated with

one nitrate and one water molecule. The enhanced relaxivity of the gadolinium ions makes Gd-PT1 suitable for selective and sensitive magnetic resonance (MR) responses towards biomolecular imaging. The distance between two metal ions bridged by one linker is 10.5 Å, and two diagonal metal ions are distant approximately by 14.9 Å. The average inner volume was estimated to 400 $Å^3$.[23] Similarly, the metal tunable isostructural nanocages based on Zn(II), Co(II) and lanthanides with the amide incorporated quinoline or pyridine derivatives have been designed possessing void volumes of approximately 400 - 500 $Å^3$. The cage windows and host-guest interactions make them attractive for the selective sensing of monosaccharides and ribonucleosides.[14, 24]

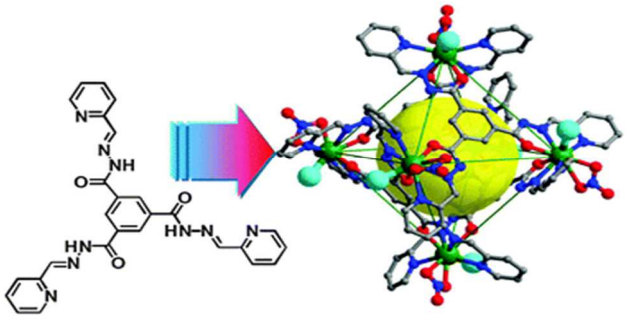

Fig. 6. Structure of the pyridine derivative (PT1) and the constitutive/constructional fragments of the gadolinium octahedron (Gd-PT1), showing the triangle opening and the coordinated water molecules (large cyan balls). Reproduced from ref. 23.

Discrete cuboctahedral cage geometry has been observed for the specific coat protein complex-II (COPII: an export machinery at endoplasmic reticulum (ER)-Golgi interface, responsible for bidirectional membrane trafficking between the ER and the Golgi,). COPII is a type of vesicle coat assembly of proteins *i.e.,* SEC13–SEC31 and SEC24–SEC23 subcomplexes).[25, 26] Similar to the SEC13-SEC31 heterotetramer assembly units arranged at vertex point, C_4 symmetric square-planer metallic nodes have been used to construct the abiological cuboctahedral cages. Examples of these cages include the combination of Pd(II) ions and metallic paddlewheel clusters with bend ditopic C_2 symmetric ligands like 4,4'-benzene-1,3-diyldipyridine[27] and benzene 1,3-dicarboxylic acid,[16] respectively (Fig. 7).

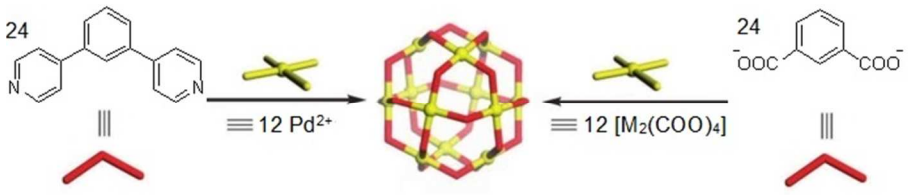

Fig. 7. Cuboctahedral cage formation based on C_4 symmetric square-planer metallic nodes like Pd^{2+} ions and metallic paddlewheel clusters ($[M_2(COO)_4]$, where M=Cu(II), Mo(II), or Rh(II) *etc.*) *etc.* and bend ditopic C_2 symmetric ligands like 4,4'-benzene-1,3-diyldipyridine or benzene 1,3-dicarboxylate linkers, respectively.

Simple substitution at the convex position of the ligand backbone *i.e.,* central phenyl ring, results in the assembly having 24 identical functional groups aligned at the cages periphery. This imparts certain properties of size as well as stability to the cage structure in a given environment. In the case of Pd(II)-based cuboctahedron, the cage diameter is around 3.5 nm. Fujita *et al*., reported $Pd_{12}L_{24}$ cuboctahedra obtained from derivatives of 4,4'-benzene-1,3-diyldipyridine functionalized with biomolecules.[13, 28] These nanoballs coated with bio-molecular moieties like DNA or saccharides are attractive as molecular devices for well-defined interactions in biological systems. These modular bio-MOP cages may serve to standardize or optimize various parameters of the biochemical phenomena to well understand the mechanisms. Furthermore, in addition to the exohedral functionalization of $Pd_{12}L_{24}$ spherical complexes, the endohedral functionalization provides the feasibility to manage the hydrophobic or hydrophilic environment. Benzene 1,3-dicarboxylic acid, H_2(1,3-BDC), and its 5-substituted derivatives generates the cuboctahedral cage formulation $[(M_2)_{12}(5\text{-R-}1,3\text{-BDC})_{24}]$ of internal cage cavity volume about 1 nm^3. Depending upon the functional groups (R), these metal-carboxylate cuboctahedra can be further modified or surface functionalization.[16] Therefore, post synthetic modification along with their use as secondary building blocks (SBBs) for the construction of respective MOFs makes them more attractive materials. Cu(II) and Rh(II) cuboctahedral cages of amino,[29] dodecyloxy,[30, 31] prop-2-ynyloxy,[32, 33] sodiumsulfonato,[34] and thymine[35] substituted 1,3-BDC derivatives have

successfully been addressed for the biochemical investigations (cationic transport through the formation of synthetic ion channels, drug delivery agents, modular interactions involving nucleobase pairs).

The angular orientation among the donor groups in the ligand is the dominating driving force for the result of discrete metal based self-assembling. A change in the bend angle of the ligand among the coordination sites (*i.e.* nitrogen and oxygen in bis(pyridine) and dicarboxylic motifs, respectively) provided by the rigid aromatic spacing, changes the geometry and size of the MOP self-assembly from the cuboctahedron to other polyhedral dimensions. Interestingly, variation in the distinct Archimedean polyhedral arrangements of the COPII cages have been observed to allow for a range of COPII vesicle carriers necessary to accommodate various cargo sizes. The combination of structural approaches has revealed that the moderate variations in geometries of subunit interactions in the SEC31 hinge bend angle (135°–165°) as well as in the β-vertex angle (90°–108°) of the SEC13–SEC31 heterotetramer subunits direct the structural change of the COPII polyhedral cages of distinct orders.[25, 26] Following the structural flexibility of the COPII cage, nanoscale cages of Pd(II) ions have been established with the bottom up construction by using curved bridging bis(pyridine) ligands. These coordination spheres follow the general cages formula $[M_nL_{2n}]$, here *n* is an integer and may vary from 6 to 60. These cages are extremely sensitive to the bend angle of ligands, because slight increment in the bend angle (4,4'-benzene-1,3-diyldipyridine and 4,4'-thiene-2,5-diyldipyridine have a bend angle of 120° and 149°, respectively) entirely changes the cage ensemble from $M_{12}L_{24}$ to $M_{24}L_{48}$ as shown in Fig. 8. However, the bend angle among the donor sites in 4,4'-(1*H*-pyrrole-2,5-diyl)dipyridine is 135° and it forms $M_{24}L_{48}$ instead of $M_{12}L_{24}$. The threshold angle for size of multicomponent assembly driven by Pd(II) ions is described as $131° < \theta < 134°$. The cage $M_{24}L_{48}$ is rhombicuboctahedral

with a 5 nm diameter circumscribed and 3.6 nm diameter inscribed sphere defining the molecular shell.[36]

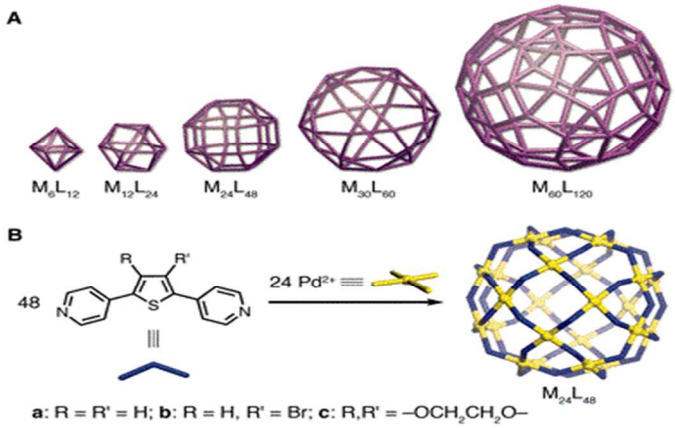

Fig. 8. (**A**) The family of M_nL_{2n} polyhedral cages (metals (M) and bridging ligands (L) are mapped onto the vertices and edges, respectively). (**B**) Self-assemblies of $M_{24}L_{48}$ rhombicuboctahedron. From ref. 36. Reprinted with permission from AAAS.

Similarly, in the case of angular ditopic carboxylic linkers having various angles (0°, 60°, 90°, and 120°) with a square four-connected node (metallic PW) realize different type of geometries (lantern-type structures (M_4L_4), trigonal (M_6L_6), octahedral ($M_{12}L_{12}$), cuboctahedral and anti-cuboctahedral ($M_{24}L_{24}$), respectively) as shown in Fig. 9.[16]

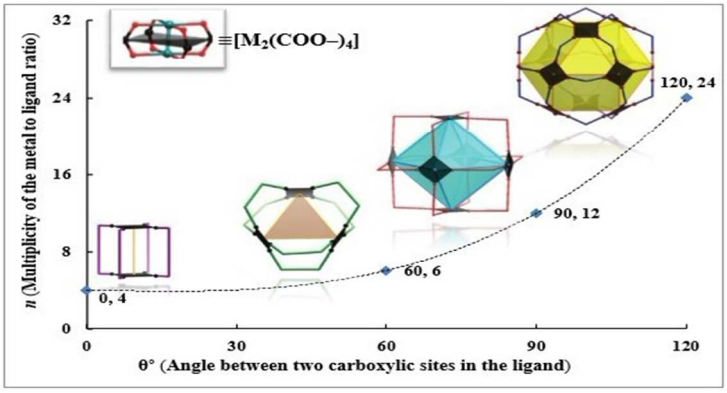

Fig. 9. The modular family of metal-carboxylate self-assembled cages built from dinuclear paddlewheel (PW) cluster $[M_2(COO–)_4]$, where metals (M) and angular ditopic bridging ligands (colored lines) are mapped onto the vertices and edges, respectively. Reprinted with permission from ref. 16.

2.2. Synthesis

Self-organization is conveniently achieved by linking metal ions with donor ligands under the given conditions of suitable solvent system, temperature, and pressure. Synthetic protocols of

solvothermal, reflux, along with the ambient conditions are mostly followed. The spontaneous reaction of metallic and ligand precursors having so small activation energy barrier, that can even be crossed at room temperature, has been observed in the case of transition metal cages of carboxylic, Schiff-base, and/or pyridine based ligands. Sometimes, simple heating over room temperature is required. Pd(II)-bispyridyl based cages are synthesized and characterized in dimethylsulfoxide at 70 °C for given time scale, ranging from 0.5 to 24 h.[36] Fe-PI cages (Fig. 1) are prepared by mixing iron(II) salt and respective amines and aldehydes in acetonitrile for 24 h at 50 °C following the addition of diisopropyl ether.[18, 19] However, choosing the suitable solvent system is the most sophisticated step for self-assembling followed by the crystallization process. Criteria for the proper solvent system are to fulfill the solubility of starting materials and maintain the reasonable rate of evaporation. For example, Ce-based cages of H_6TTS, H_8TBDS, and H_8TBBS are obtained by diffusing methanol to their respective solutions with $Ce(NO_3)_3 \cdot 6H_2O$ in DMF.[21, 22] The block crystals of Gd-PT1 cage were obtained in $CH_3OH/CHCl_3$.[23] Similarly, crystals of the cuboctahedral cages of copper(II) having amino,[29] dodecyloxy,[30] prop-2-ynyloxy,[33] sodiumsulfonato,[34] and thymine[35] *etc.* functional moieties substituted BDC linkers are obtained at room temperature using an appropriate solvent system. However, the synthesis under the room temperature conditions takes several days to obtain crystallization. Hence, to speed up the process, the solvothermal method is also a reasonable approach. While in this case along with solvent parameters, reaction temperature, holding time and the chemical reactivity *vs* pressure are crucial for the product morphology and crystallinity.[16, 20, 32]

3. Ionic transport

Flow of inorganic ions is regulated by the ion channels to support the cellular life. To understand the mechanistic details and operational features of the natural ion channels, artificial analogues are designed. Like biological channels, single-molecular synthetic ion channels (SICs) based on conducting structures permit fluxes of same magnitude. Therefore, SIC are *de novo* chemical formulations arising from macromolecular entities based on crown ethers, calixarenes, cyclodextrins, peptides, and metal-organics *etc*., inserted into lipid bilayers allowing the passage of ions across the pores.[37] In 2001, Fyles and coworkers described a synthetic ion channel from low molecular weight compounds (alkoxy substituted isophthalic acid derivatives) in the absence of any metal ions. 5-(12-tricosanoxy)-isophthalic acid embedded in a planar and vesicle bilayer membrane formed quite stable channels that showed Ohmic properties and low conductance, and exhibited selectivity for alkali metal ions ($Cs^+ > K^+ > Na^+$).[38] By the use of macromolecules containing metal-organic scaffolds for the creation of ion channels and pores it is quite possible to access the ultrastable nanospace.[39] This approach is acknowledged to stabilize the confined space within the pores based on internal charge repulsion between residues on the inner pore surfaces.[40] Incorporating properly designed and modified self-assemblies into lipid bilayers systems imitates the natural channels, which could serve in both technological and diagnostic roles. Novel ion-channel systems with rigid structure, accessible at ambient conditions, and tunability of the size and chemical environment of pores can show significant functional regularity including stability and ion's selectivity. SIC supported by nanosized self-assembled metal-organic polyhedra are developed and subjected to the ionic transport activity for proton and alkali metal ions through the windows to the cavity. The latter has resulted in new technological aspects and therapeutics.

The ionic transport and single molecule detection behavior by metal-organic polyhedral cages are of great interest. Furukawa *et al.* synthesized a charge-neutral MOP-18, $[(Cu_2)_{12}(5\text{-dodecyloxy-1,3-BDC})_{24}]$, with overall size of 5 nm having a hydrophilic cuboctahedral core cavity (diameter of 13.8 Å), which is accessible through 8 triangular and 6 square windows each with a diameter of 3.8 Å and 6.6 Å, respectively.[30] An unprecedented synthetic ion channel derived from MOP-18 (Fig. 10) has successfully been used to transport protons and alkali-metal ions across the lipid membranes (EYPC-LUVs; egg yolk phosphatidylcholine large unilamellar vesicles).[41] Different models like Goldman-Hodgkin-Katz and Michaëlis-Menten were tested for the transport analysis. Proton transport through the membranes was measured by the change in fluorescence intensity of the pH sensitive dye HPTS (8- hydroxypyrene-1, 3, 6-trisulfonate) that was entrapped inside the vesicles. The cation transport activity of MOP-18 decreases according to the following order $Li^+ >> Na^+ > K^+ > Rb^+ > Cs^+$. The high selectivity for Li^+ followed the Eisenman sequence XI, suggesting that binding of ions to the channel is more crucial than dehydration in the ion transport making the ion-channel very unique. Whereas, other synthetic ion channels mostly follow Eisenman sequences I–IV (weak field-strength sequences).[42] The initial rate of Na^+ transport increases linearly with the mole fraction of MOP-18 indicating that single molecule constitutes the ion channel.[41]

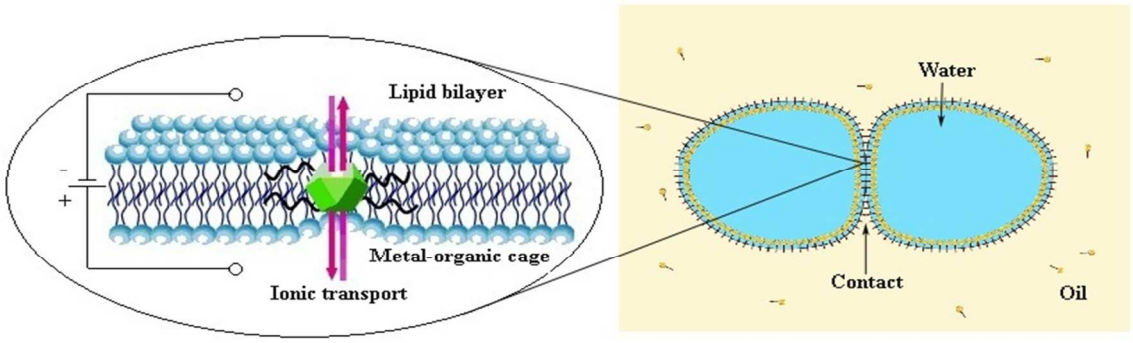

Fig. 10. Schematic diagram of synthetic ion channel (SIC). Metal-organic cage embedded in a bilayer lipid membrane, prepared by the droplet contact method. Copyright © 2008 Wiley-VCH Verlag GmbH & Co. KGaA, Weinheim.

Similar to MOP-18, the rhodium-organic cuboctahedron $[(Rh_2)_{12}(5\text{-dodecyloxy-1,3-BDC})_{24}]$ (C14RhMOP) having nanopores of 0.6 nm, obtained from $Rh_2(OAc)_4(MeOH)_2$ and H_2(5-dodecyloxy-1,3-BDC) embedded by the droplet contact method into a bilayer of the lipid membrane has been studied electro-physiologically. From the single channel current analysis, the long-lived open-and-closed transitions revealed a channel conductance of 36 pS. Ion permeability of C14RhMOP was observed by saturation of the single channel conductance at high KCl concentration. Changing the alkali metal, transport activity gave the following sequence: $Li^+ > Na^+ \approx K^+ > Rb^+$. This predicted that binding of the cations to the channel is more crucial than dehydration of the cations in the ion transport.[31]

Similar to cationic transport, there is also the possibility to follow the anionic transport using the metal-organic self-assemblies. In this regard Nitschke *et al.* have established cationic M(II)-cages which offer differential binding affinities for a set of anions. The binding studies of different anions (perchlorate (ClO_4^-), tetrafluoroborate (BF_4^-), hexafluorophosphate (PF_6^-), trifluoromethanesulfonimide (triflimide, NTf_2^-) and triflate (OTf^-)) through the host-guest mechanism were performed. The results of binding affinities revealed that Fe-PI cages are selective to bind the anions. The anion binding trend for Fe-PI1 is $ClO_4^- > BF_6^- > OTf^- > PF_4^- > NTf_2^-$. Whereas in the case of Fe-PI2, it follows a different trend *i.e.* $ClO_4^- > PF_6^- > OTf^- > BF_4^-$.

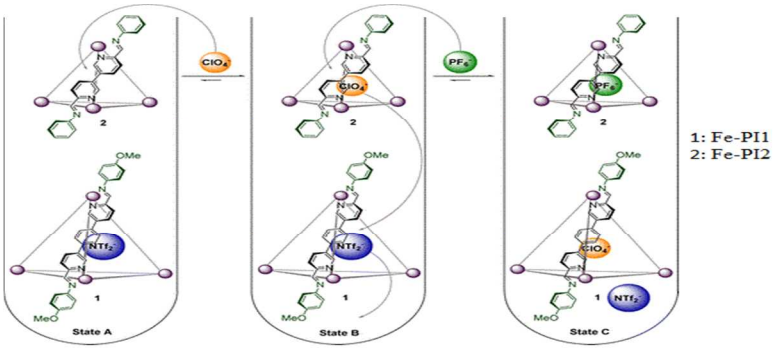

Fig. 11. Anion exchange sequence: binding of ClO_4^- within Fe-PI2, followed by its displacement by PF_6^-, and subsequent displacement of NTf_2^- from Fe-PI1 by the released ClO_4^-. Reprinted with permission from ref. 19. Copyright 2013 American Chemical Society.

However, no binding was observed for NTf_2^-, as its volume (157 $Å^3$) would render it too large to serve as a guest in Fe-PI2**.** More interestingly, in the presence of a multi anionic environment there is competitive ion encapsulation according to the size of both the cage cavity and the anion as well. Thus, the addition of PF_6^- caused that perchlorate had to shift from Fe-PI2 to cage Fe-PI1, and NTf_2^- was ejected from Fe-PI1 into the solution (Fig. 11).[19] Therefore, these types of cages observed the selectivity internally; dynamic interchange demonstrated by guest anions *i.e.* either by the diffusion *via* open faces of the cage assisted by twisting of the ligands, or by the dissociation of the ligands, involves Fe–N bonding within the range of 10^{-5}-10^{-6} s^{-1}. This dynamic selective anion binding along with reconfigurable exterior may lead to the development of suitable recognition or signaling systems providing specific responses to the applied stimuli in the biological systems.[18, 19]

Custelcean *et al.,*[43] reported novel urea based tetrahedral M_4L_6 cages of Zn(II) and Ni(II) in the presence of a templating tetrahedral oxoanion (EO_4^{n-}) under aqueous conditions (Fig. 12). The unusual encapsulation of such strongly hydrophilic anions ($M_4L_6 \supset EO_4^{n-}$) is stabilized by the twelve hydrogen bonds. The guest (anion) exchange experiments revealed that M_4L_6 cage have different binding affinities and selectivities for different oxoanions. The selectivity trend among the tetrahedral anions is: $PO_4^{3-} \gg CrO_4^{2-} > SO_4^{2-} > SeO_4^{2-} > MoO_4^{2-} > WO_4^{2-}$. Factors which may contribute to the difference in selectivity include anion size, charge, hydration, H-bond acceptor ability and basicity.[43]

Fig. 12. Self-assembly of anion templated M_4L_6 cages of Zn(II) and Ni(II). Reprinted with permission from ref. 43. Copyright 2013 American Chemical Society.

Browsing the idea from nature, introducing such systems, which may readjust themselves according to the environment, would be a great deal. The metal-organic cages capable to express the complex responses to the specific chemical signals, *i.e.* second order templations, may consider their performance like natural biochemical systems. Riddell *et al.*[20] has characterized the Co_4L_6 (L: 3,3'-bipyridine-6,6'-diylbis(methanylylidene)bis(4-methylaniline) tetrahedron capable of an ion (perchlorate) induced structural transformation into an unprecedented $Co_{10}L_{15}$ pentagonal prism having strong binding for other ions (chloride). Herein, the initial single anion binding event triggers the structural reorganization (template effect) creating a highly efficient binding pocket for another ion (allosteric effect). Therefore, metal-organic cages capable of undergoing spontaneous reconstitution and introducing new functions in a given environmental stimuli would be attractive and will reflect biological systems.

4. Molecular recognition and imaging

The molecular recognition refers to a specific interaction between two or more molecules through noncovalent bonding such as hydrogen bonding, metal coordination, hydrophobic forces, Van der Waals forces, π-π interactions, halogen bonding, electrostatic and/or electromagnetic effects. In addition to these *direct* interactions as well the solvent can play a dominant indirect role in driving molecular recognition in solution. Molecular recognition plays an important role in biological systems, an important example of molecular recognition is the antibiotic vancomycin that selectively binds with the peptides with terminal D-alanyl-D-alanine in bacterial cells through five hydrogen bonds. The vancomycin is lethal to the bacteria since, once it has bound to these particular peptides, they are unable to be used to construct the bacteria's cell wall. Specially designed artificial supramolecular systems can exhibit molecular recognition. Functional moieties in the ligands impart certain desirable properties like photophysical properties for the given biochemical protocols. More specifically, special functional groups in MOPs are selected to match with particular molecular species present in the

targeted systems which may be *in vivo* or *in vitro*. Luminescent cages can be used for molecular detection and to better understand the physiological processes for trapped compounds. Beside this, symmetry, stability, biocompatibility and biodegradability of MOPs make the task more attractive. Therefore, MOPs have a great potential in biochemistry owing to solution stability and properties in specific experimental conditions and chemical environment like acidic, basic, sensing species, and temperature *etc.*[7-9]

Binding studies based on host-guest chemistry have dominated the field of molecular recognition. MOPs can play a role of molecular sensors due to their several significant features for example spatial selection resulting from cavity size, tuning the hydrophobicity incorporated hydrogen bond acceptor and donor sites, *etc*. The exact situation entirely depends upon the particular structure which gives various physicochemical functionalities and the sensing target. In the last decade, rapid developments of multifunctional self-assembly design and applications are recognized. Cage structures *e.g.* Werner-type capsules having novel and notable properties have been developed, because they give a selective signal responses when applied for sensing special guests.[44] The size, shape, selectivity, and dynamic self-assemblies are utilized for molecular recognition highlighting the detection and collection of easy-to-measure signals from amplifying guest-bonding events.[45]

Molecular sensing has come up as a growing research area, and macromolecular systems as chemosensory application of resisting diseases are given high attentions. Arene-Ru-based supramolecular coordination complexes formed *via* [2+2] metalla-cage assembly are selectively sensitive to rigid anionic molecules like oxalate anion, where notable photophysical changes occurred. As well, oxalate exchange disruption is recognized as a mark for several diseases, so it is a significant biological oxyanion, but it is insensitive to monoanionic species such as acetate or

halide ions. Further it is not only oxalate but also tartrate and citrate are highlighted due to their importance in various biological processes, connected by strong interactions with self-assembly.[46-48]

Well-confined MOP self-assemblies including adjustable lipophilic features exhibiting biocompatibility and cell permeability[39] are handy for the application to biomolecular imaging and detection. MOP functionalization with amide groups, the characteristic structural motif of a protein, could be a useful attempt to achieve functional metal-organic polyhedra with suitable hydrophilic/lipophilic characteristics. A robust neutral cerium-based tetrahedron Ce_4-H_2TTS (Fig. 4) incorporates a triphenylamine moiety with three amide groups (H_6TTS) often used as a bright blue emitter, is emphasized as a luminescent detector of 2-phenyl-4,4,5,5-tetra-methylimidazolineyloxyl-3-oxide (PTIO) which is a specific spin-labeling nitric oxide (NO) trapper. The tetrahedral cage encapsulated molecules of NO and PTIO prompt the spin-trapping reaction and transforms the normal EPR responses into a more sensitively luminescent signaling system with the detection limit improved to 5 nM.[21]

The presence of other reactive species like H_2O_2, $^1O_2$, ClO^-, NO^{2-}, NO_3^-, and $ONOO^-$ does not disturb the probing process. Moreover, this MOP system is able to respond to NO in aqueous media at physiological pH range (5.0-9.0). Therefore, encapsulation of spin-trapping agent PTIO within the cavities of the luminescent MOP provides a new probing method with significantly improved selectivity over the traditional systems, Fig. 13. Kinetics of the spin trapping between PTIO and NO is second order (k, 5.15×10^3 $M^{-1}s^{-1}$) and under the saturation conditions exhibit a pseudo-zeroth-order kinetic behavior. This is typically like the enzymatic Michaelis-Menten mechanism in which substrate binding is the rate-limiting step of the reaction. Twelve-fold functionalized amide groups in the tetrahedron, to modify the hydrophilic environment, ensure

the successful application of biological imaging in living cells (MCF-7). Ce-H_2TTS system is used for monitoring intracellular NO, and is the first example of the applicability of metal-organic polyhedra for biological imaging in living cells. The cells display blue luminescence after 30 min incubation at room temperature by self-assembly. The cells remained viable throughout the imaging experiments (about 3-4 h).[21]

Fig. 13. Structure of the Ce-H_2TTS functional tetrahedron showing the sequence of fluorescent variation of the tetrahedron upon the addition of PTIO and NO. Reprinted with permission from ref. 21. Copyright 2011 American Chemical Society.

Interestingly, the molecular cage Ce–H_2TTS, also demonstrated a high selectivity and sensitivity towards quantificational detection of tryptophan (Trp) over all other natural amino acids and Trp-containing peptides (*in vitro*). The detection mechanism involved interactions within cage cavity supported by the synergistic effects of H-bonding, π-stacking and size/shape matching. This enabled the successful use of Ce–H_2TTS in biological imaging of Trp in living cells and application for serum Trp-content detection. Advance developments may ultimately lead to application of the methodology in the clinical detection and monitoring of intracellular Trp.[49]

A Ce-based octanuclear bicoronal triangular prism and tetranuclear molecular tetrahedron with the ligands *N*,*N*′-bis(3,5-bis(2-(2-hydroxybenzylidene)hydrazinecarbonyl)phenyl) terephthalamide (H_4TRBS) and *N*,*N*′,*N*″-tris(4-(2-hydroxybenzylidene)hydrazinecarbonyl) phenyl)benzene-1,3,5-tricarboxamide (H_3TBAS), containing 36 and 24 folds amides, respectively within their main backbones were achieved. These two new Ce-cages have been

structurally characteristics for the selective luminescent recognition of disaccharides with the highest sensitivity for lactose. According to the Hill-plot from emission spectra, both Ce-TRBS and Ce-TBAS MOPs exist as 1:1 complexation host–guest species in the solution with lactose and sucrose, respectively (Fig. 14). The fluorescence spectrum generated by the spatial selectivity for lactose and the weak interaction of hydrogen bonds between the lactose/sucrose and Ce-MOPs as artificial receptor can only be obtained by the specifically discrimination over other disaccharides. The ESI-MS spectrum of Ce-TRBS and Ce-TBAS upon the addition of lactose and sucrose exhibited new peaks at *m/z*=2408.58 and 1565.84 suggesting the presence of $[(Ce_6^{III}Ce_2^{IV}(TRBS)_6 \supset (lactose)\text{-}5H]^{3-}$ and $[(Ce\text{-}TBRS)\text{-}3H \supset (sucrose)(CH_3CN)_3]^{3-}$, respectively. Therefore, Ce-based coordination polyhedra serve as efficient selective chemosensors for special natural saccharides.[50]

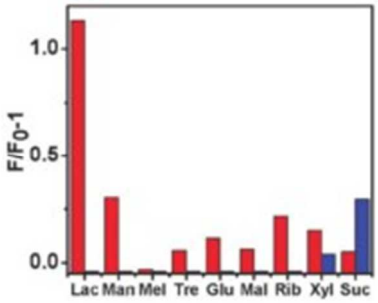

Fig. 14. Fluorescence responses of Ce-TRBS (red bars) and Ce-TBAS (blue bars) for saccharides (emission intensity was recorded at 424 nm for Ce-TRBS or 435 nm for Ce-TBAS (20 mM in DMF/acetonitrile (1:9, v/v), excited at 315 and 340 nm, respectively). Reproduced from ref. 50.

Molecular cubes Ce-TBDS and Ce-TBBS (Fig. 5) have shown luminance recognition of saccharides. The addition of mono- and disaccharides caused a significant fluorescence enhancement while the Hill plot profile of the fluorescence titration curve at 465 nm demonstrated a 1:2 stoichiometric host–guest behavior (K_{ass}, ranging 1.15–5.37×10^5 M^{-1}) for the monosaccharides (ribose, xylose, and glucose), and a 1:1 stoichiometric host–guest behavior (K_{ass} 0.62–1.20 × 10^3 M^{-1}) for the disaccharides (lactose, maltose, and sucrose). The ESI-MS

spectra of Ce-TBBS in the presence of disaccharides exhibited new peaks at *m/z*=1850.62 and 1860.19, corresponding to $[Ce_8(H_2TBBS)_2(H_3TBBS)_4\supset(C_{12}H_{22}O_{11})]^{4-}$ and $[Ce_8(H_2TBBS)_3(H_3TBBS)_3\supset (C_{12}H_{22}O_{11})K]^{4-}$, respectively. This confirmed the formation of 1:1 stoichiometric host–guest complexation species in solution and established the recognition applications based on the fluorescent photo-induced electron transfer (PET) mechanism[51] of these lanthanide molecular cages in luminescent carbohydrate sensing. From a mechanistic viewpoint, the formation of donor-type hydrogen bonds between the amide groups and the guest molecules could alter the electronic distribution of the ligand backbone, leading to the significant luminescence enhancement. However, the low selectivity toward the tested saccharides (Fig. 15) indicated that the carbohydrate receptor frameworks are large enough to fully encapsulate an oligosaccharide nucleus, but did not have suitable sequence of pre-organized inward-directed H-bonding sites to enable the specificity.[22]

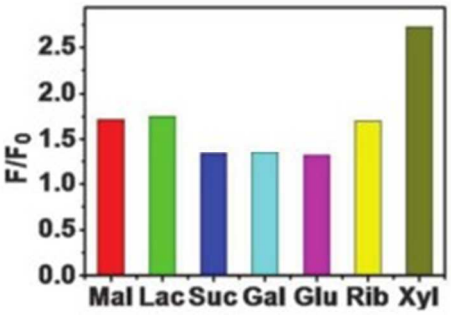

Fig. 15. Fluorescence responses of Ce-TBBS (1×10^{-5} M) in DMF solution upon the addition of various saccharides (0–10 mM, excited 340 nm). Reproduced from ref. 22.

Another illustration of a well-established molecular recognition procedure through a metal-organic cage is the bio-MOP made from Pd(II) ions and pyridine-containing ligand functionalized by a family of saccharides giving a MOP surface decoration by 24 clustered saccharide molecules (sac-MOP) at once (Fig. 16). Molecular recognition between saccharide clusters at the surface of MOPs and saccharide-binding proteins induced a cross-linking of the

soluble proteins resulting in the formation of colloidal aggregates. Concanavalin A (ConA: lectin from *CanaValia ensiformis*) selectively recognizes *α*-mannopyranoside and *α*-glucopyranoside at its four binding sites. In accordance, the cages bearing 24 *α*-mannopyranoside units at its periphery served as a cross-linker for ConA and supports aggregation in solution of DMSO and HEPES (*4-(2-hydroxyethyl)-1-piperazineethanesulfonic acid*) buffer. Whereas, upon addition of an excess amount of *α*-methyl mannopyranoside as an inhibitor against the sac-MOP, the opaque solution returned almost clear, which is due to disaggregation of the sac-MOP-ConA aggregate. Similarly, when peanut agglutinin (PNA: a galactose-binding lectin from *Arachis hypogaea*) was used, MOP bearing *β*-galactopyranoside coagulated and was analyzed by turbidity measurement. Therefore, clustered saccharides on the spherical platform of MOP are an efficient mode for binding to ConA or PNA recognizing the conformation of the saccharides and the combination of the protein recognition at the periphery. Conversely, the similar molecular functionalization at the interior of the spheres will also lead to many biochemical applications.[28]

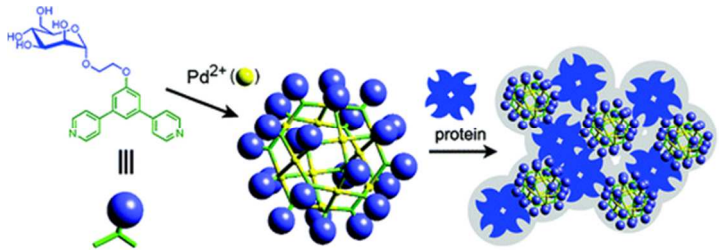

Fig. 16. Self-assembly of $Pd_{12}L_{24}$ cage functionalized with α-mannopyranoside at the periphery providing a pathway to interact with proteins. Reprinted with permission from ref. 28. Copyright 2007 American Chemical Society.

Thymine as a functional moiety has been reported as the first nucleobase-incorporated metal-carboxylate cuboctahedron. In the thymine-incorporated assembly (TMOP), $[Cu_{24}$(5-((5-methyl-2,4-dioxo-3,4-dihydropyrimidin-1(*2H*)-yl)methyl)isophthalate$)_{24}(DMA)_4(H_2O)_{20}]$ as shown in Fig. 17, the open hydrogen bonding sites in the nucleobase create the potential to integrate DNA base pair interactions. This shows the potential in making DNA coated biosensors and it is progressive research with respect to the biological applications of material science. This will give

an attractive call for these nanocages as nucleobase-incorporated biosensors and further use in biomedical science providing more options to explore for other MOPs.[35]

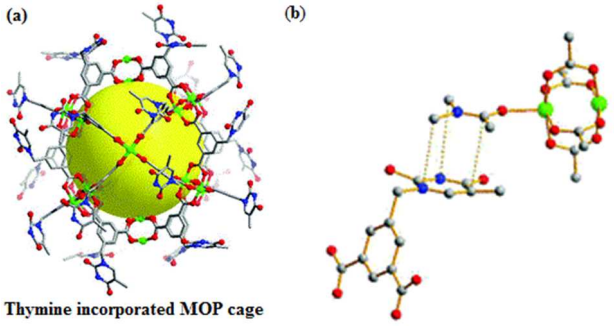

Fig. 17. (**a**) The crystal structure of thymine-incorporated Cu(II) MOP cage. The yellow sphere indicates the empty space inside its cage. All the coordinating solvents are omitted for clarity. (**b**) The π···π interaction between the coordinating DMA and a neighboring thymine facilitates the packing of the MOP. The grey, red, blue and green spheres/nodes represent C, O, N and Cu, respectively. H atoms are omitted for clarity. Reproduced from ref. 35.

Introduction of biomolecules into the chemical composition of the cage can provide a platform for certain biochemical applications. Therefore, DNA-coated nanospherical cages may serve as biological sensors in DNA/RNA detection, gene regulation, and biological screening. The surface-functionalized Pd(II)-MOPs bearing well-defined, perfectly monodisperse 24 short DNA oligonucleotides strands at the convex of the pyridine based bidentate ligands are capable to interact and selectively recognize oligonucleotides, Fig. 18a. Based on the diffusion coefficient, the estimated cage diameter of **2c** is 4.5 nm, which is still larger than that of the core framework (3.5 nm) indicating that the peripheral DNA strands are not fully extended otherwise it would optimize around 8.7 nm. This cage served as a nanoparticle template to control the number, spacing, and alignment of the peripheral DNA strands. The deoxythymine (T) based Pd(II) cage showed specific binding to the complimentary nucleotide deoxyadenosine (A). The binding of Pd(II)-MOP (T) nucleotides to the added nucleotide (A) was monitored in solution through NMR measurements following changes in proton chemical shifts, as shown in Fig. 18b. The peripheral DNA strands of **2c** formed Watson-Crick base pairs with complementary oligodeoxyadenosine trimers (tri-A). For the mixture of tri-A **3c** and **2c** the signals of the thymine amide protons

shifted downfield (Δδ=0.06 ppm) forming base pair between T and A. The plot of the downfield shifting as a function of the equivalent guest strands shows the chemical shift of thymine protons which in turn clearly implies the selective recognition of complementary oligonucleotide by using the oligonucleotide-coated sphere *via* hydrogen bonds. The DNA coated nanocages recognized and selectively formed hydrogen bonds with the complementary nucleobases. These results display that oligonucleotide-modified spheres afford promising materials as a new recognition platform for natural DNA in aqueous media.[13]

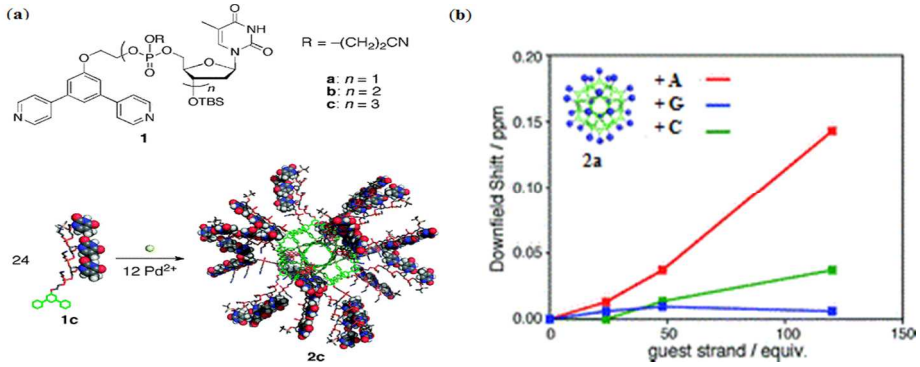

Fig. 18. (**a**) Structures of ligands**1a-c**. Self-assembly of DNA-conjugated molecular sphere. (**b**) The value of downfield shift of thymine proton signals of **2a** after the addition of complimentary oligonucleotide nucleic bases ($Pd_{12}L_{24}$=0.167 mM, DMSO-d_6/$CDCl_3$=1:4, 500 MHz, 300 K). Reprinted with permission from ref. 13. Copyright 2010 American Chemical Society.

In the Pd(II) octahedron based on ligand QL_1 (Fig. 19), upon addition of one molar equiv of uridine, the d_6-DMSO molecules within the cages were replaced with the uridine (U) molecules. ESI-MS results showed a 1:1 stoichiometric host–guest complexation species. While upon adding other RNA-based nucleosides, namely guanosine (G), cytidine (C), and adenosine (A), no peaks associated with the host–guest complexes were found. Moreover, the fluorescence spectra exhibited about 90% enhancement in the emission intensity when uridine was added into the solution and lower enhancement in case of G, C (both 30%), and A (20%). The difference in the fluorescence responses is assigned to the different interaction patterns between the nucleic bases and the Pd(II)-octahedra. The presence of amide groups is likely to enhance the strength of

hydrogen bonds between nucleotides and the cage receptor, which may certainly correspond to the fluorescence enhancement of the cage in response to nucleoside C is greater than that to A, and the enhancement pertaining to U is higher than that to G (Fig. 20B). Since, the hydrogen bonds with the type of O···H–N are always stronger than that of N···H–N. The quinoline group serves as a fluorophore constituting the nitrogen donor for assembling the Werner-type cages. The amide groups act promptly to the efficient guest interactions and efficient binding-signaling transduction that transforms the recognition information into the fluorescent signals. Hence, the Pd(II) MOP based on the ligand QL_1 with three amide groups showed selective recognition of U over the other nucleosides (U≫G≈C>A).[52]

Metal–organic octahedra of cobalt, zinc and lanthanides derived from QL_2 and PL_3 are tested as artificial chemosensors for selective detection of glucosamine[14] and ribonucleosides[24] in solution. Two-fold hydrogen bonds between the base of the corresponding ribonucleosides and the interaction sites in the MOP make the nanocages adaptive receptors for selective sensing of cytidine or uridine over other nucleotides. Cobalt and zinc cages of QL_2 exhibited a different role in the recognition of a series of ribonucleosides. The organic linkers in these cages which incorporate three (CONHN=CH) moieties presented selective interaction with cytidine. The inclusion behaviour of the cytidine molecule within the inner space of the positively charged cage is most likely because of the special two-fold hydrogen bonding pattern involving the CH group (Fig. 20A) which only occurs between the C and the cage. Hence, selectivity is C≫G>A>U.[24] Interestingly, while Co(II)-QL_2 showed interactions with the amino sugar glucosamine, it revealed no interaction at all with glucose. Significant changes in absorbance or λ_{max} in UV/Vis spectra and the chemical shift values in ^{1}H-NMR revealed the selectivity of these

octahedra towards guests, whereas in the case of glucosamine, the presence of glucose did not have any effect.

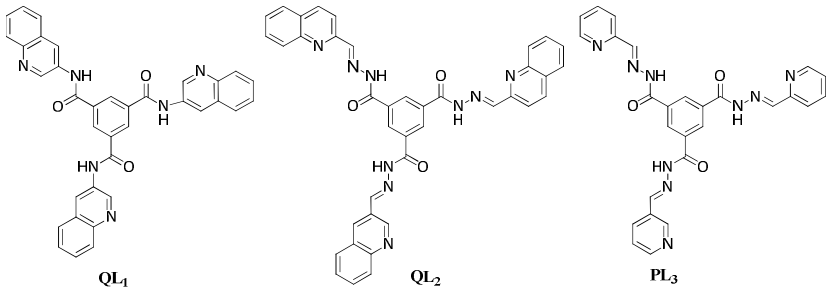

Fig. 19. Ligand structures QL_1, QL_2 (quinolone derivatives), PL_3 (pyridine derivative) incorporating amide moieties for designing MOP with nucleosides recognition activity.

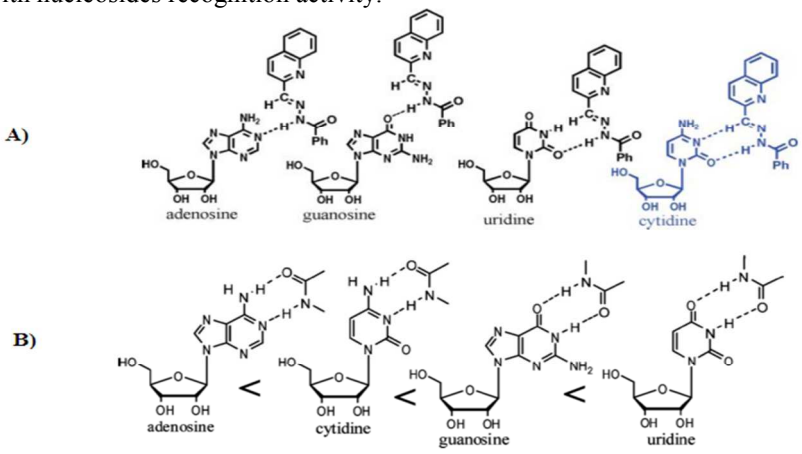

Fig. 20. The potential two-fold hydrogen bonds between the amide groups which are present as functional moieties in the metal-organic self-assemblies and the nucleic bases **A**) cytidine, and **B**) uridine. Reproduced from ref. 24.

The presence of three sharp isosbestic points ≥ 300 nm disclosed that only two species coexist in the equilibrium. ESI-MS data demonstrated the evidence of a 1:1 stoichiometric host (MOP) and guest (glucosamine) complexation also reinforcing the UV/Vis data with association constant ($\log K_{ass}$) values ranging from 4.5 to 5.6. Moreover, the coordination of Zn(II), blocked the photo-induced electron transfer (PET) between quinolone and the amide groups resulting in the fluorescence enhancement and simultaneously opens a photo-induced charge transfer (PCT) channel. Also, the delocalization reduces the energy of the highest occupied molecular orbital (HOMO) due to hydrogen bonding between amide functions and guest molecules further supported blocking of the PET giving an extra push to metal-tunable luminescence signal.[14]

The robust hexanuclear gadolinium octahedral cage using pyridine instead of quinolone moieties furnished the rigid facial planar bridging ligand (PT1, Fig. 6) providing an additional boost for the proton relaxivity around gadolinium ions ensuring the application of magnetic resonance imaging (MRI) *in vivo*. Simple gadolinium complexes with one metal center and one coordinated water molecule having a non-rigid structure show much low relaxivity (r_1 =4.5 $mM^{-1}s^{-1}$; 20 MHz, 298 K) relative to the theoretically attainable maximum. While in Gd-PT1 octahedra, each of the six Gd centers strongly bonded to the four rigid planar ligands and coordinated water, exhibited quite high longitudinal relaxivity (r_1=388.5 $mM^{-1}s^{-1}$) with small longitudinal relaxation time (T_1=5.14 ms) corresponding to 64.8 $mM^{-1}s^{-1}$ per Gd center. The water exchange rate (k_{ex}) at the Gd center is about 1.1 × 103 s^{-1}, assessed by the well-established VT ^{17}O-NMR analysis.[23] Gd-MOP as hypodermic injection (0.5 mM, DMF/H_2O (v/v, 10/1)) into a rat performed excellent selectivity on the MR responses towards glucosamine (as indicated by the significant changes in r_1 and T_1) over glucose and other tested ribonucleosides (U, C, G, and A), Fig. 21. A mechanistic approach affirmed that the decrease in the longitudinal relaxivity could be attributed to the coordination of glucosamine that replaced the coordinated water (Fig. 6). Further, luminescence responses enhancement of Eu-PT1 by the addition of 10 equiv. glucosamine leads to the conclusion that the lanthanide octahedra could be described as the glucosamine-specific probes based on *in vivo* MR responses. In this regard, the excellent selectivity of Gd-PT1 on the MR responses towards glucosamine over glucose and ribonucleosides (Fig. 21c) is a milestone. These results gave a breakthrough in the field of clinical radiology and in biomedical imaging techniques enabling diagnosis, monitoring the disease, and treatment profile as well.[23]

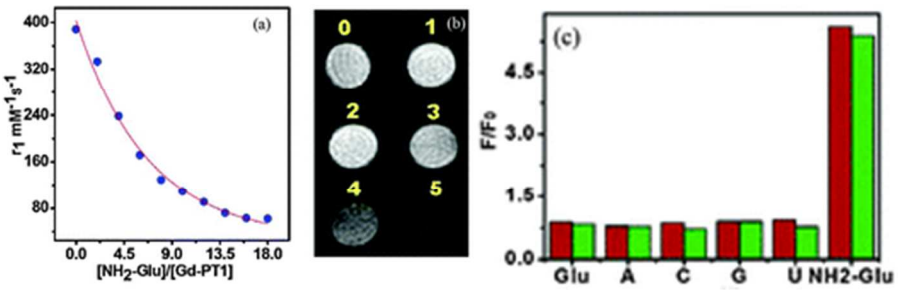

Fig. 21. (**a**) Proton relaxivity responses of Gd-PT1 (0.5 mM) in 1:10 (v : v) water–DMF solution towards NH_2-Glu (Glu: glucosamine) at various concentrations with 400 MHz magnetic field at 298 K. (**b**) Longitudinal relaxation time T_1-weighted *in vivo* (for rat) MRIs of Gd-PT1 (0.5 mM) incubated with NH_2-Glu (1: 0 mM, 2: 0.5 mM, 3: 1.5 mM, 4: 3 mM, 5: 7 mM at 20 MHz field). (**c**) The normalized longitudinal relaxation times of Gd−PT1(0.5 mM) in 1:10 (v:v) water–DMF solution (red bars) and the normalized luminescence of Eu−PT1 (0.02 mM) in 1:20 (v:v) water–acetonitrile solution (green bars) at 615 nm upon the addition of 9 mole ratio ribonucleotide or glucose, excitation at 365 nm. Reproduced from ref. 23.

5. Pharmaceutical applications

Drug delivery to specific locations within the human body using material-based systems occupied the forefront of biomedical research for the past few decades. Development of new materials for the well-controlled drug delivery systems remains a challenging task. It is always encouraging to enhance and enable a new life to the existing drugs by exploiting new routes of administration. Recently, metal-organic self-assemblies with proper functionalities and appealing drug hosting and release potential are a new input to the field. Analogous with enzymes and other large biomolecular systems for encapsulating guest(s) in a confined environment, it is advantageous to use the MOP self-assemblies which offer storage, carrier and then controlled release. Precise surface decoration and hence functionalization with long aliphatic hydrocarbon chain to get amphiphilic and biocompatible supramolecular self-assemblies could achieve an anticipated environment for drug loading and release. Moreover, metal-organic cages have the potential to selectively encapsulate the molecules based on the size of the cage cavity. For the drug delivery studies, it is important to load the drug into a third party carrier agent and then get the release as per required. The release of encapsulated guest molecules from the cage cavity is the working mechanism for the drug delivery. Therefore, in the light of this it is very attractive

that self-assembled cages have the immense potential to be used in pharmaceutics as drug vectors and delivery agents.

Ruthenium(II) complexes have been investigated extensively as potential anticancer drugs, and it is well established that the presence of more lipophilic arene ligands increases the uptake at the expense of selectivity. Pyrene derivatives are known to intercalate between base pairs of DNA, interfere with transcription, and allows monitoring of uptake and intracellular localization due to its fluorescence properties, that can be exploited to design anticancer drugs. Unfortunately, incorporation of the pyrenyl moiety into the structure of a drug could alter its water solubility, which is required in order to achieve higher cellular uptake. Discrete metal-organic assemblies were exploited to combine a DNA intercalator (pyrene moiety) connected to the arene ligand of arene ruthenium metal-based and in the same time maintaining the drug water solubility to increase the cellular uptake. The pyrenyl group was encapsulated in the hydrophobic cavity of the large water-soluble metalla-cage. An important feature of this type of metalla-assemblies is their susceptibility to selectively target cancer cells and increase cellular uptake through the EPR effect.[53] Floxuridine has been utilized as potent anticancer drug; however, its therapeutic effect is limited by the efficiency of cellular uptake and bioavailability of the drug. In order to overcome these limitations, several approaches have been explored to enhance the cell permeability and cytotoxicity of floxuridine derivatives as potent anticancer drugs. In this regard, the pyrene moiety was functionalized with floxuridines resulting in pyrenyl-nucleoside derivatives. Thereafter, the water-soluble arene ruthenium metalla-cages were used to deliver pyrenyl-nucleosides to cancer cells.[54] Additionally, different pyrenyl-arene based ruthenium complexes of the general structure [Ru(η^6-arene-pyrenyl)Cl_2(1,3,5-triaza-7-phosphaadamantane)] functionalized *via* alkane chains containing ester, ether and amide functional groups were

encapsulated through the pyrenyl moieties into the hydrophobic cavity of water soluble metal-organic cage with ruthenium ends pointing out. These host-guest systems [drug⊂cage]$(CF_3SO_3)_6$ displayed good anticancer activity (IC_{50} range 2-8 μM after 72 h exposure) as evaluated *in vitro* in different types of human cancer cell lines. These results are a good therapeutic alternative to pyrenyl-arene ruthenium complexes and floxuridine which suffers from poor cellular uptake and bioavailability.[55]

The prototype ionic self-assembly (ISA) unit $[Cu_{24}(5SO_3\text{-isophthalate})_{24}]^{24-}$ is surface functionalized with the dimethyl distearyl ammonium chloride (DODAC) cationic surfactant. Micelle like nanoparticles, about 3 nm in diameter, having a well-defined spherical structural integrity of the polyhedral cages and without dissembling during the electrostatic self-assembling between MOP anion and DODAC (1:1) are recognized. This post synthetic modification may serve as a foundation for highly ordered and controlled organization of nanocages to use them in the domain of biophysical science and is quite capable for storage and delivery applications of the encapsulation of drug.[34]

Caffeine is a widely used stimulant drug, its release profile has been investigated for the self-assembly derived from Cu(II) paddlewheels and 5-(prop-2-ynyloxy)isophthalic acid (pi). The encapsulation of caffeine as a guest inside the cage cavity was performed by stirring their DMF solutions at room temperature, and by recrystallization from EtOAc. In this way, the suitable loading of caffeine molecules (ca. 4.85%) inside the cage cavity was observed. The reduction in the surface area of the caffeine loaded MOP, confirmed encapsulation in the core instead of just adsorption on the surface. The release plot patterned like sustained delivery of cavity-trapped caffeine; this outcome is based on gradual departure of the loaded drug from the pores to the aqueous media. Hence, the caffeine loaded metal-organic self-assembly was exposed into water

and the induced conversion mechanism of the cage stimulated the controlled/gradual release over time (Fig. 22).[32]

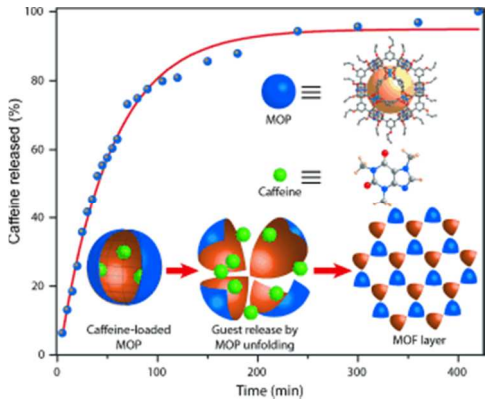

Fig. 22. Release profile of encapsulated caffeine molecules from the self-assembly derived from Cu(II) paddlewheels and 5-(prop-2-ynyloxy)isophthalic acid. A schematic representation of the release driven by the unfolding event is also shown. Copyright © 2013 Wiley-VCH Verlag GmbH & Co. KGaA, Weinheim.

The alkyne-covered surface of the coordination sphere has also been functionalized through click reaction with azide terminated polyethylene glycol (N_3-PEG5K). The reaction product was well characterized and revealed that the dicopper paddlewheel cluster remains intact and thus maintaining the MOP periphery during the click reaction modification. The surface functionalized cages carry at the maximum 3-4 chains of PEG5K and they were found to be useful as a drug delivery agent (Fig. 23a).[33] This surface functionalized porous coordination nanocage of Cu(II) and 5-(prop-2-ynyloxy)isophthalic acid (pi) bearing polymer (PEG5k) material has successfully been applied as a drug delivery agent for anticancer drug 5-Fluorouracil (5-FU) in aqueous media. A loading of 5-FU into Cu(pi)-PEG5k of 4.38 wt% was obtained based on the solubility difference of 5-FU between chloroform and methanol. Drug release analysis was performed by dialyzing the drug loaded MOP (Cu(pi)-PEG5k⊃5-FU) in a phosphate-buffered saline solution (pH 7.4) at room temperature. Pure 5-FU was also dialyzed as a control experiment, in which almost the entire drug (90%) was released within 7 hours. Whereas, in case of Cu(pi)-PEG5k⊃5-FU, less than 25% of the loaded drug was released during

the initial burst release (2 hours) followed by a much sustained curve up to 24 hours. The initial fast release may come from the drug that was imbedded within the entangled polymeric chains at the MOP periphery. The rest of the drug, loaded within the Cu(pi) core and/or the void between nearby Cu(pi) cores, was released very gently. This slow release profile is related to the slow diffusion rate of 5-FU caused by the strong interaction between Lewis acid sites in Cu(pi) and basic site in 5-FU.[33]

The system based on the stepwise assembly of metal–organic framework [Cu_{24}(5-NH_2-isophthlate)$_{24}$(bipyridine)$_6$(H_2O)$_{12}$] derived from [Cu_{24}(5-NH_2-isophthlate)$_{24}$] cuboctahedron was also explored for drug release. Around 80% of the loaded drug was released during the initial fast-release (7.5 h), Fig. 23b. Furthermore, degradation of the stepwise assembly structure probably causes a fast release. Nevertheless, lateral slow release of the remaining 20% encapsulated drug may be loaded inside the individual cage cavities rather than being entrapped between the spaces among MOP building units created during the construction of stepwise assembly. Therefore, the sustained release of a drug is promising feature of self-assembly systems.[29]

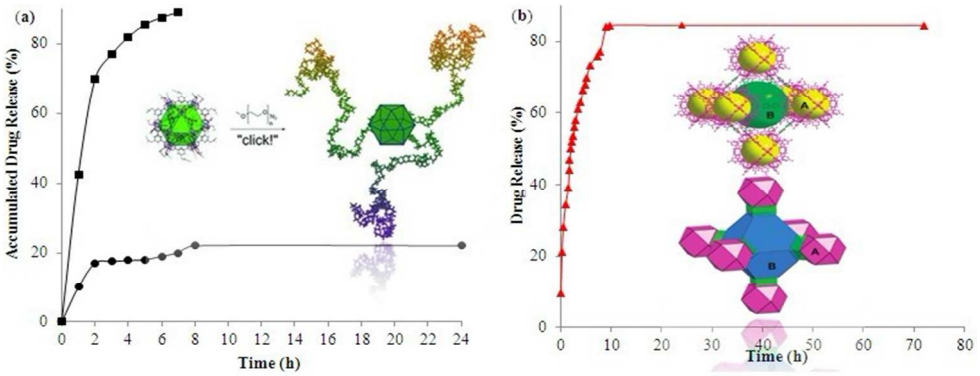

Fig. 23. Drug release profiles of 5-fluorouracil (5-FU) from; (**a**) surface functionalized cage Cu(pi)-PEG5k (circle) and control (square), Copyright © 2011 Wiley-VCH Verlag GmbH & Co. KGaA, Weinheim, (**b**) the two types of cages (A and B) in [Cu_{24}(5-NH_2-isophthlate)$_{24}$(bipyridine)$_6$(H_2O)$_{12}$], reproduced from ref. 29.

6. Conclusion and future prospects

Abiological metal-organic self-assemblies are promising for the continual development and use as emerging materials with a worth of applications. The rationally designed structural features provide dynamic/static, geometric, coordinative, and functional properties to the cage-like architectures. Metal-organic molecular cages are establishing their impact on the biochemical investigative protocols. A number of biochemical processes are regulated *via* the ionic transport of cations as well as anions. In this scenario, the development of the metal-organic cage based synthetic ion channels, anion selective binding studies and chemical reconstitution of self-assembled cages are reliable forums to better understand and further control the related biochemical processes. Metal-organic scaffold and given organic functional moieties are efficient probes to act as signaling units, guest interactions sites, and communicators for success of artificial chemosensors. The selective luminescent recognition of saccharides and nucleosides by the metal-organic cages are exclusive. Similarly, the results of biomolecular imaging of NO and glucosamine by the amide containing cerium tetrahedron and gadolinium octahedron are a breakthrough in the field of clinical science. The saccharide or nucleobase incorporated molecular spheres have evidenced their direct interaction with proteins and DNA. Moreover, the utilization of the molecular cages as drug carrier and delivery agents is undoubtedly a remarkable achievement by these materials.

To optimize the performance of metal-organic molecular cages in the biochemical investigations, a number of factors should be considered. The rational design having a specific functionality and biocompatibility for molecular cage assembly in a mild bio-functional way can interact with the biomolecules either on the surface or with in the cage cavity. Other signal transduction methods *e.g.* magnetic, electrochemical, mechanical, and other physical properties, suitable for a given molecular cage irrespective of its properties and structure would provide a pace progress to the

expansion and more opportunities in this field. Thus, in future the tailored metal-organic polyhedral cages are expected to show more promising applications as bio-analytical tools.

Acknowledgements

The authors would like to express their deep appreciation to Chinese Scholarship Council (CSC) for the financial support to N.A., H.A.Y., and A.H.C. for their PhD grants 2012GXZ641, 2012GXZ639 and 2013GXZ988, respectively. F.V., acknowledges the Chinese Central Government for an ‘‘Expert of the State’’ position in the program of ‘‘Thousand talents’’ and the support of the Natural Science Foundation of China (No. 21172027).

References

1. J. J. Perry Iv, J. A. Perman and M. J. Zaworotko, *Chem. Soc. Rev.*, 2009, **38**, 1400-1417.
2. T. R. Cook, Y.-R. Zheng and P. J. Stang, *Chem. Rev.*, 2012, **113**, 734-777.
3. S. Chaemchuen, N. A. Kabir, K. Zhou and F. Verpoort, *Chem. Soc. Rev.*, 2013, **42**, 9304-9332.
4. R. J. Kuppler, D. J. Timmons, Q.-R. Fang, J.-R. Li, T. A. Makal, M. D. Young, D. Yuan, D. Zhao, W. Zhuang and H.-C. Zhou, *Coord. Chem. Rev.*, 2009, **253**, 3042-3066.
5. P. Horcajada, R. Gref, T. Baati, P. K. Allan, G. Maurin, P. Couvreur, G. Férey, R. E. Morris and C. Serre, *Chem. Rev.*, 2011, **112**, 1232-1268.
6. D. J. Tranchemontagne, Z. Ni, M. O'Keeffe and O. M. Yaghi, *Angew. Chem. Int. Ed.*, 2008, **47**, 5136-5147.
7. K. Harris, D. Fujita and M. Fujita, *Chem. Commun.*, 2013, **49**, 6703-6712.
8. Z. Lu, C. B. Knobler, H. Furukawa, B. Wang, G. Liu and O. M. Yaghi, *J. Am. Chem. Soc.*, 2009, **131**, 12532-12533.
9. C. M. Vetromile, A. Lozano, S. Feola and R. W. Larsen, *Inorg. Chim. Acta*, 2011, **378**, 36-41.
10. M. Zhang, Z.-Y. Gu, M. Bosch, Z. Perry and H.-C. Zhou, *Coord. Chem. Rev.,* 2014, http://dx.doi.org/10.1016/j.ccr.2014.05.031.
11. L. E. Kreno, K. Leong, O. K. Farha, M. Allendorf, R. P. Van Duyne and J. T. Hupp, *Chem. Rev.*, 2011, **112**, 1105-1125.
12. M. Yoshizawa, J. K. Klosterman and M. Fujita, *Angew. Chem. Int. Ed.*, 2009, **48**, 3418-3438.
13. T. Kikuchi, S. Sato and M. Fujita, *J. Am. Chem. Soc.*, 2010, **132**, 15930-15932.
14. C. He, Z. Lin, Z. He, C. Duan, C. Xu, Z. Wang and C. Yan, *Angew. Chem. Int. Ed.*, 2008, **47**, 877-881.
15. M. M. Smulders, I. A. Riddell, C. Browne and J. R. Nitschke, *Chem. Soc. Rev.*, 2013, **42**, 1728-1754.
16. N. Ahmad, A. H. Chughtai, H. A. Younus and F. Verpoort, *Coord. Chem. Rev.*, 2014, **280**, 1-27.
17. M. J. Prakash and M. S. Lah, *Chem. Commun.*, 2009, 3326-3341.

18. Y. R. Hristova, M. M. J. Smulders, J. K. Clegg, B. Breiner and J. R. Nitschke, *Chem. Sci.*, 2011, **2**, 638-641.
19. S. Ma, M. M. Smulders, Y. R. Hristova, J. K. Clegg, T. K. Ronson, S. Zarra and J. R. Nitschke, *J. Am. Chem. Soc.*, 2013, **135**, 5678-5684.
20. I. A. Riddell, M. M. Smulders, J. K. Clegg, Y. R. Hristova, B. Breiner, J. D. Thoburn and J. R. Nitschke, *Nat. Chem.*, 2012, **4**, 751-756.
21. J. Wang, C. He, P. Wu, J. Wang and C. Duan, *J. Am. Chem. Soc.*, 2011, **133**, 12402-12405.
22. L. Zhao, S. Qu, C. He, R. Zhang and C. Duan, *Chem. Commun.*, 2011, **47**, 9387-9389.
23. C. He, X. Wu, J. Kong, X. Zhang and C. Duan, *Chem. Commun.*, 2012, **48**, 9290-9292.
24. Y. Liu, X. Wu, C. He, Z. Li and C. Duan, *Dalton Trans.*, 2010, **39**, 7727-7732.
25. F. Brandizzi and C. Barlowe, *Nat. Rev. Mol. Cell Biol.*, 2013, **14**, 382-392.
26. C. Gurkan, S. M. Stagg, P. LaPointe and W. E. Balch, *Nat. Rev. Mol. Cell Biol.*, 2006, **7**, 727-738.
27. M. Tominaga, K. Suzuki, M. Kawano, T. Kusukawa, T. Ozeki, S. Sakamoto, K. Yamaguchi and M. Fujita, *Angew. Chem. Int. Ed.*, 2004, **43**, 5621-5625.
28. N. Kamiya, M. Tominaga, S. Sato and M. Fujita, *J. Am. Chem. Soc.*, 2007, **129**, 3816-3817.
29. H.-N. Wang, X. Meng, G.-S. Yang, X.-L. Wang, K.-Z. Shao, Z.-M. Su and C.-G. Wang, *Chem. Commun.*, 2011, **47**, 7128-7130.
30. H. Furukawa, J. Kim, K. E. Plass and O. M. Yaghi, *J. Am. Chem. Soc.*, 2006, **128**, 8398-8399.
31. R. Kawano, S. Furukawa, D. Kiriya, T. Osaki, K. Kamiya, S. Kitagawa and S. Takeuchi, "Synthetic nanocage formed by rhodium-organic cuboctahedra: For single molecule detection in lipid bilayer", Solid-State Sensors, Actuators and Microsystems (TRANSDUCERS & EUROSENSORS XXVII), 2013 Transducers & Eurosensors XXVII: The 17th International Conference, pp. 854-855, IEEE, 16-20 June 2013, Barcelona, SPAIN, doi: 10.1109/Transducers.2013.6626901.
32. A. Mallick, B. Garai, D. D. Díaz and R. Banerjee, *Angew. Chem. Int. Ed.*, 2013, **52**, 13755-13759.
33. D. Zhao, S. Tan, D. Yuan, W. Lu, Y. H. Rezenom, H. Jiang, L. Q. Wang and H. C. Zhou, *Adv. Mater.*, 2011, **23**, 90-93.
34. Y. Li, D. Zhang, F. Gai, X. Zhu, Y.-n. Guo, T. Ma, Y. Liu and Q. Huo, *Chem. Commun.*, 2012, **48**, 7946-7948.
35. M. Zhang, W. Lu, J.-R. Li, M. Bosch, Y.-P. Chen, T.-F. Liu, Y. Liu and H.-C. Zhou, *Inorg. Chem. Front.*, 2014, **1**, 159-162.
36. Q.-F. Sun, J. Iwasa, D. Ogawa, Y. Ishido, S. Sato, T. Ozeki, Y. Sei, K. Yamaguchi and M. Fujita, *Science*, 2010, **328**, 1144-1147.
37. G. W. Gokel and S. Negin, *Acc. Chem. Res.*, 2013, **46**, 2824-2833.
38. T. M. Fyles, R. Knoy, K. Müllen and M. Sieffert, *Langmuir*, 2001, **17**, 6669-6674.
39. N. Sakai and S. Matile, *Angew. Chem. Int. Ed.*, 2008, **47**, 9603-9607.
40. V. Gorteau, G. Bollot, J. Mareda, D. Pasini, D.-H. Tran, A. N. Lazar, A. W. Coleman, N. Sakai and S. Matile, *Bioorg. Med. Chem.*, 2005, **13**, 5171-5180.
41. M. Jung, H. Kim, K. Baek and K. Kim, *Angew. Chem. Int. Ed.*, 2008, **47**, 5755-5757.
42. A. L. Sisson, M. R. Shah, S. Bhosale and S. Matile, *Chem. Soc. Rev.*, 2006, **35**, 1269-1286.

43. R. Custelcean, P. V. Bonnesen, N. C. Duncan, X. Zhang, L. A. Watson, G. Van Berkel, W. B. Parson and B. P. Hay, *J. Am. Chem. Soc.*, 2012, **134**, 8525-8534.
44. K. Harano, S. Hiraoka and M. Shionoya, *J. Am. Chem. Soc.*, 2007, **129**, 5300-5301.
45. A. P. De Silva, H. N. Gunaratne, T. Gunnlaugsson, A. J. Huxley, C. P. McCoy, J. T. Rademacher and T. E. Rice, *Chem. Rev.*, 1997, **97**, 1515-1566.
46. V. Vajpayee, Y. H. Song, M. H. Lee, H. Kim, M. Wang, P. J. Stang and K. W. Chi, *Chem. Eur. J.*, 2011, **17**, 7837-7844.
47. N. Morakot, W. Rakrai, S. Keawwangchai, C. Kaewtong and B. Wanno, *J. Mol. Model.*, 2010, **16**, 129-136.
48. R. Pal, D. Parker and L. C. Costello, *Org. Biomol. Chem.*, 2009, **7**, 1525-1528.
49. C. He, J. Wang, P. Wu, L. Jia, Y. Bai, Z. Zhang and C. Duan, *Chem. Commun.*, 2012, **48**, 11880-11882.
50. Y. Jiao, J. Zhang, L. Zhang, Z. Lin, C. He and C. Duan, *Chem. Commun.*, 2012, **48**, 6022-6024.
51. T. Gunnlaugsson, M. Glynn, P. E. Kruger and F. M. Pfeffer, *Coord. Chem. Rev.*, 2006, **250**, 3094-3117.
52. Y. Liu, X. Wu, C. He, R. Zhang and C. Duan, *Dalton Trans.*, 2008, 5866-5868.
53. M. A. Furrer, F. Schmitt, M. Wiederkehr, L. Juillerat-Jeanneret and B. Therrien, *Dalton Trans.*, 2012, **41**, 7201-7211.
54. J. W. Yi, N. P. Barry, M. A. Furrer, O. Zava, P. J. Dyson, B. Therrien and B. H. Kim, *Bioconjugate Chem.*, 2012, **23**, 461-471.
55. J. Mattsson, O. Zava, A. K. Renfrew, Y. Sei, K. Yamaguchi, P. J. Dyson and B. Therrien, *Dalton Trans.*, 2010, **39**, 8248-8255.